Contributions to Tobacco & Nicotine Research
formerly: Beiträge zur Tabakforschung International
Volume 31 · No. 3 · November 2022
DOI: 10.2478/cttr-2022-0014

Thermal De-Oxygenation to Form Condensable Aerosol From Reconstituted Tobacco without Auto-Ignition *

by

Zhongya Guo [1], Shiyu Wang [1], Ke Zhang [1], Ping Lei [2], Lili Fu [1], Qi Zhang [1], Shanzhai Shang [2], Shuang Wang [1], Le Wang [1], Mingjian Zhang [1], Weimin Gong [2], Jingmei Han [2], Zhiqiang Li [2], Yonghua Pan [2], Feng Huang [1], Chuan Liu [1], Jianguo Tang [1], Bing Wang [1], and Bin Li [1]

[1] *Zhengzhou Tobacco Research Institute of CNTC, Zhengzhou 450001, Henan, China*
[2] *China Tobacco Yunnan Industrial Co. Ltd, Kunming 650202, Yunnan, China*

SUMMARY

A novel concept is described here that utilizes externally applied heat to a solid rod of reconstituted tobacco biomass to form a stream of aerosol under progressively oxygen-deficient atmosphere. The boundary of auto-ignition was determined at oxygen concentrations of 0%, 5%, 10%, and 21% and then the effects of these different atmospheres on various parameters were studied. Experimental results indicated that the ignition temperature decreased with the increase of oxygen concentration and a negative temperature coefficient (NTC) for atmosphere with oxygen was observed at before but close to ignition temperature. Significant differences in the yields of CO and CO_2 between oxygen and oxygen-free atmosphere were observed. The mass of aerosol produced under an inert atmosphere and reduced-oxygen atmosphere were characterized with selected volatile and semi-volatile components, phenols, aldehydes, and other organic compounds of interests. In addition, higher oxygen concentration resulted in higher bulk and surface oxygen content of solid-phase residue, the reduction of carbon and hydrogen element content and related functional groups, and the content of inorganic compounds also exhibited an increase with oxygen concentration. By systematically changing oxygen concentrations of the biomass bed with increasing temperatures, an aerosol stream of controlled chemical composition and yields could be formed without leading to ignition. Key chemical markers of inhalation harm were measured and compared to each other under different degrees close to combustion. Studying reconstituted tobacco or other biomass materials in such a way could provide alternative and useful information in the design heated biomass aerosol generators. [Contrib. Tob. Nicotine Res. 31 (2022) 130–141]

KEYWORDS:

Oxygen concentration; auto-ignition; aerosol; solid-phase residue; inorganic compounds

ZUSAMMENFASSUNG

In diesem Artikel wird ein neuartiges Konzept beschrieben, bei dem einem festen Strang aus rekonstituierter Tabakbiomasse von außen Hitze zugeführt und dabei in einer zunehmend sauerstoffarmen Atmosphäre/Umgebung ein Aerosolstrom erzeugt wurde. Die Grenze der Selbstentzündung wurde bei Sauerstoffkonzentrationen von 0%, 5%, 10% und 21% bestimmt. Anschließend wurden die Auswirkungen dieser unterschiedlichen Atmosphären auf verschiedene Parameter untersucht. Die Versuchsergebnisse zeigten, dass die Zündtemperatur mit zunehmender Sauerstoffkonzentration sank. Unterhalb aber in der Nähe

*Received: 24th January 2022 – accepted: 30th June 2022

This work is licensed under a Creative Commons Attribution-NonCommercial-ShareAlike 4.0 International License (CC BY-NC-SA 4.0).
© 2022 Authors who publish with this journal retain all copyrights and agree to the terms of the above-mentioned CC BY-NC-SA 4.0 license.

der Zündtemperatur wurde in der sauerstoffhaltigen Atmosphäre zudem ein negativer Temperaturkoeffizient (NTK) beobachtet. Es wurden signifikante Unterschiede bei den Ausbeuten an CO und CO_2 zwischen der sauerstoffhaltigen und der sauerstofffreien Atmosphäre festgestellt. Die Masse des jeweils unter inerter und sauerstoffreduzierter Atmosphäre erzeugten Aerosols wurde anhand von ausgewählten flüchtigen und halbflüchtigen Bestandteilen, Phenolen, Aldehyden und anderen organischen Verbindungen von Interesse bestimmt. Eine höhere Sauerstoffkonzentration führte zudem zu einem höheren Gesamt- und Oberflächensauerstoffgehalt im Festphasenrückstand sowie zu einer Verringerung des Gehalts an Kohlenstoff- und Wasserstoffelementen und der entsprechenden funktionellen Gruppen. Auch der Gehalt an anorganischen Verbindungen nahm mit der Sauerstoffkonzentration zu. Durch die systematische Änderung der Sauerstoffkonzentration im Biomassebett bei zunehmender Temperatur konnte ein Aerosolstrom mit kontrollierter chemischer Zusammensetzung und Ausbeute erzeugt werden, ohne dass es zu einer Entzündung kam. Die wichtigsten chemischen Marker für Inhalationsschäden wurden gemessen und bei verschiedenen Graden nahe der Verbrennungstemperatur miteinander verglichen. Eine derartige Analyse von rekonstituiertem Tabak oder anderen Biomassematerialien könnte somit zusätzliche und nützliche Erkenntnisse für die Entwicklung von Aerosolerzeugern für erhitzte Biomasse liefern. [Contrib. Tob. Nicotine Res. 31 (2022) 130–141]

RESUME

Le présent article détaille un concept novateur d'application externe de chaleur à un boudin solide composé de biomasse de tabac reconstitué dans le but de produire un flux d'aérosols dans une atmosphère ou un environnement progressivement appauvrie en oxygène. La limite d'auto-inflammation fut déterminée à des concentrations en oxygène de 0%, 5%, 10% et 21% avant que ne soient ensuite étudiés les effets de ces atmosphères variées sur de multiples paramètres. Les résultats de ces expériences indiquèrent que la température d'inflammation chutait lorsque la concentration en oxygène augmentait et un coefficient de température négatif (CTN) dans une atmosphère alimentée en oxygène fut observé à un point proche mais juste inférieur à la température d'inflammation. Des écarts significatifs au niveau des rendements de CO et de CO_2 furent notés entre les atmosphères alimentées en oxygène et celles qui en étaient exemptes. La masse d'aérosols produite dans une atmosphère inerte et dans une atmosphère pauvre en oxygène fut déterminée sur la base d'une sélection de composés volatiles et semi-volatiles, de phénols, d'aldéhydes et d'autres composés organiques présentant un intérêt. En outre, il s'avéra qu'une concentration plus élevée en oxygène provoquait une augmentation de la teneur totale en oxygène et de la teneur en oxygène à la surface des résidus de phase solide, une réduction de la teneur en éléments carbonés et hydrogénés et des groupes fonctionnels afférents; la teneur en composés inorganiques grimpait également suivant la concentration en oxygène. En modifiant systématiquement la concentration en oxygène du lit de biomasse et en relevant la température, un flux d'aérosols présentant des rendements et une composition chimique contrôlés put être produit sans provoquer un phénomène d'inflammation. Les marqueurs chimiques essentiels de nocivité par inhalation furent mesurés et comparés les uns aux autres à différents degrés proches de la combustion. L'étude du tabac reconstitué ou d'autres matières sous forme de biomasse suivant ce protocole pourrait fournir une méthode alternative et des informations utiles pour la conception de générateurs d'aérosols à biomasse chauffée. [Contrib. Tob. Nicotine Res. 31 (2022) 130–141]

1. INTRODUCTION

The presence of harmful and potentially harmful constituents (HPHCs) in the smoke resulting from burning tobacco is well known (1–4). Technology research to reduce the level of toxic smoke compounds has been carried out worldwide, and these technologies are expected to be applied to produce potentially reduced-risk products (5). Based on the generation mechanism of smoke compounds, one effective way to develop technologies for the reduction of toxic compounds is to try to suppress tobacco combustion.

In the 1980s, the R.J. Reynolds Tobacco Company (USA) developed a cigarette that heated tobacco rather than burned it. The cigarette generated a much simpler smoke chemistry than conventional cigarettes in a non-burning state. The smoke gave significantly lower responses in a variety of bioassays and generated less sidestream smoke than conventional cigarettes (1, 6). The R.J. Reynolds Tobacco Company subsequently developed the "heat but not burn" tobacco concept further and launched a modified version with reconstituted tobacco sheet mostly consisting of tobacco extracts, glycerol and flavors in 1995. In 1998 the Philip Morris Company in the USA developed a handheld device with battery-operated electric heating elements for a cigarette that heated tobacco rather than burned it. Toxic chemicals (relevant to smoking-related diseases) in smoke were reduced by at least 80% (7). The total particulate matter from the electrically heated cigarette was up to 90% lower in mutagenicity than the reference cigarette on an equal particulate matter basis, and 40% less active in a cytotoxicity bioassay (8).

Subsequent products that used a handheld device to electrically heat a tobacco rod continued to demonstrate a significant reduction in toxicant emissions in the aerosol, and were also successful commercially (9, 10). In heating tobacco products such as PMI's *IQOS*, BAT's *glo*, Japan Tobacco's *ploom S*, and Korea Tobacco's *lil*, the heating temperature is essentially limited to render the tobacco substrate into a non-combustible state during use (11–17). In addition to pyrolysis temperature, oxygen, as one of the three major elements of combustion, is also decisive in controlling combustion. Based on the creation of a tobacco matrix low-oxygen pyrolysis environment and the establishing of a unique smoke extraction method, NSC has been constructed by B. Li *et al.* (18) to ensure that the tobacco is heated rather than ignited, NSC is a label of the novel-designed airflow pathway of heated tobacco products. Through the coordination of cigarettes and handheld devices, oxygen (or air) will not flow through the tobacco

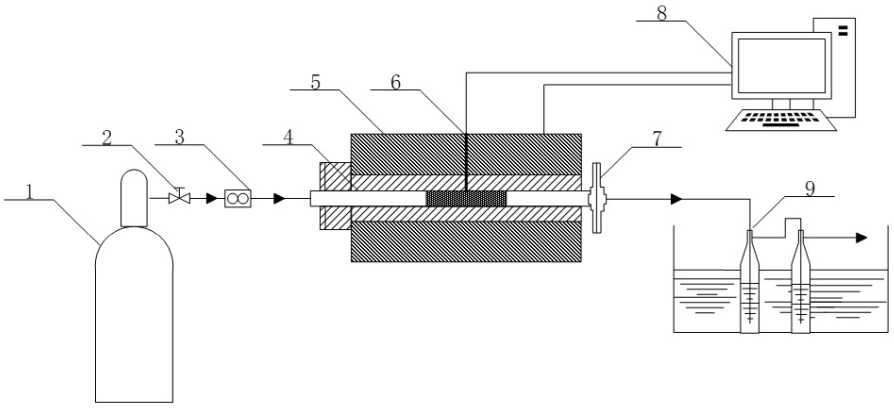


Figure 1. Scheme of aerosol generation and capture device. 1) Gas source; 2) relief valve; 3) mass flowmeter; 4) quartz tube; 5) tube furnace; 6) thermocouple; 7) Cambridge filter; 8) temperature control system; 9) cold trap.

section during the main aerosol formation and transfer process, thus the aerosol generation mechanism for NSC is fundamentally different from the current heating tobacco products, especially the pyrolysis atmosphere and the airflow pathway.

Mild oxidation (or low temperature oxidation) has been verified to show significant influence on liquid yields during pyrolysis and to change undoubtedly the aliphatic structures of fossil fuels (or biomass), although the question whether it induces the change on the aromatic structures is seen controversially (19). As a radical enhancer, oxygen facilitates the formation of free radicals (e.g., aliphatic/olefinic structures) before they are oxidized and further decomposed to produce relatively stable oxygenated products (e.g., alcohols, ketones, aldehydes, esters and ethers) as well as CO, CO_2 and H_2O (5). The hydrogen-rich components exhibit more susceptibility to oxidation than the hydrogen-poor network portion of coal (20). For tobacco pyrolysis (mainly at high temperatures even under combustion), significant influence of (oxygen and non-oxygen) atmosphere on the smoke compounds has been verified (21, 22). Formaldehyde, acrolein, isoprene and styrene showed significantly higher yields in air than in non-oxygen atmosphere. However, the effect of oxygen and oxygen concentrations on the pyrolysis products for heating tobacco at relatively low temperature, especially the aerosol compounds have not been reported.

The final aim of the study is to shed some light on the effect of oxygen concentrations on the thermal transformation process and pyrolysis product distribution of tobacco at low temperature, especially harmful smoke components, and then to provide basic and useful information to further study the formation mechanisms and the technology involved in the control of aerosol generation for heated tobacco products.

2. EXPERIMENTAL

2.1 Biomass material preparation

The biomass materials were reconstituted tobacco by papermaking method from Yunnan China Tobacco Industry Co., Ltd. They were dried at 80 °C for 2 h before being grinded and sieved to below 24 mesh.

2.2 Determination of ignition temperature

A thermogravimetric analyzer (STA 449 F3, Netzsch Gerätebau GmbH, Selb, Germany) was used to study the onset of ignition and corresponding temperatures of the prepared biomass materials at 5%, 10%, and 21% oxygen concentrations. The weight loss process of (10.0 ± 0.5) mg samples was recorded from 105 °C to 600 °C at a heating rate of 10 °C/min after removing moisture by keeping at 105 °C for 10 min. The onset of ignition was observed by the derivative thermogravimetric (DTG) curve dividing point method. The dividing point between combustion and pyrolysis on the DTG curve was recorded as the ignition point, and the corresponding temperature was the ignition temperature. Since the lowest ignition temperature was found to be 370 °C, for the rest of the investigations, the heating temperature was selected as either at or below 370 °C for this type of biomass sample.

2.3 Aerosol generation and capture

To measure the amount and the chemical composition of the aerosol formed under de-oxygenated conditions, a sample of 100 mg of prepared materials was placed in a quartz tube (150 mm in length and 8 mm in diameter); this was loaded into the constant temperature zone of a heating tube furnace (OTF-1200X-25-60, MITR, Hefei, Anhui Province, China) (Figure 1). Before each experiment, a loaded quartz glass tube was purged for 10 min by a carrier gas (see below for composition) to eliminate the influence of air. Then it was heated from 35 to 370 °C at a rate of 10 °C/min. The carrier gas was a mixture of nitrogen and oxygen with an oxygen concentration of 0%, 5%, 10% and 21% and at a flow rate of 40 mL/min. A visible aerosol stream was formed and flown out of the heating zone by the carrier gas. The aerosol stream was captured by a Cambridge filter pad (44 mm in diameter, Borgwaldt, Hamburg, Germany) at the exit. Previous studies have indicated that this filter setup is capable of capturing over 98% of aerosol particles larger than 0.5 nm in diameter (23). For volatile and a portion of semi-volatile flue gas components that escaped the capture, cold liquid traps were used behind the Cambridge filter pad system. The liquid consisted of 15 mL of an ethyl acetate/methanol (95:5 vol/vol) absorption

solution that was put under −75 °C using dry ice.
After the experiment, the Cambridge filter and the cold trap bottle were combined in a 20-mL brown bottle, sealed and ultrasonicated for 30 min, and then left to stand for subsequent analyses. The solid residuals were collected and named as S-0-O, S-5-O, S-10-O and S-21-O, respectively.

2.4 Aerosol composition analysis

Captured aerosol fractions were analyzed by a gas chromatography-mass spectrometry (GC-MS) with three separations (24) labelled as A, B and C. For A and B separations, 1 mL extract and internal standard (phenethyl acetate, 20 μg/mL) with a volume ratio of 5 mL/100 μL was analyzed with GC-MS after being filtered by a microporous membrane (0.45 μm). For separation C, a mixture of 100 μL filtrate from System A and 100 μL BSTFA derivatization reagent was analyzed by GC-MS.
Separation A used following parameters: DBWAX UI column (30 m × 0.25 mm×0.5 μm) with He as the carrier gas at a flow rate of 1.5 mL/min, an injection port temperature of 250 °C, a split ratio of 20:1, and an injection volume of 1 μL. The heating program was as follows: the initial temperature was 35 °C and held for 2 min, then increased to 200 °C at 10 °C/min and held for 2 min, then increased to 250 °C at 30 °C/min and held for 7 min.
For separation B: DB-FFAP column (30 m × 0.25 mm × 0.25 μm) with He as the carrier gas at a flow rate of 3.2 mL/min, an injection port temperature of 240 °C, a split ratio of 20:1, and an injection volume of 1 μL. The heating program was as follows: the initial temperature at 40 °C was held for 2.5 min, then increased to 150 °C at 30 °C/min, followed by an increase to 200 °C at 5 °C/min, afterwards an increase to 220 °C at 8 °C/min and being held for 2 min, then increased to 240 °C at 30 °C/min and being held for 8 min.
For separation C: DB-624 column (30 m×0.32 mm×1.8μm) with He as the carrier gas at flow rate of 1.5 mL/min, an injection port temperature of 220 °C, a split ratio of 20:1, and an injection volume of 1 μL. The heating program was as follows: the initial temperature was 60 °C and was held for 1 min, then increased to 130 °C at 15 °C/min, followed by an increase to 180 °C at 4 °C/min, then again increased to 250 °C at 20 °C/min and held for 5 min.
The mass spectrometer (7890B/5977A, Agilent Company, Santa Clara, CA, USA) was connected by a transfer line operated at 290 °C. The temperature of the electron impact (EI) ionization source was 230 °C and the temperature of the quadrupole was 150 °C. The detection mode was SCAN and SIM, and the scanning range was 25 ~ 400 amu.
Peak identification was made by using the NIST standard library (version 2.3). The retention time and qualifier ions (Table 1) were used to quantify the determined compound. The peak area of the internal standard substance was set at 1, and the ratio of the peak area of the target compound to that of the internal standard substance was used as the relative content of the target compound.

2.5 Solid residual characterization

Scanning electron microscopy (SEM) was performed on the solid residual after the heating of biomass samples (S-4800, Hitachi, Tokyo, Japan). It was operated at 1 kV, and the solid residual was Au-coated first under vacuum. X-ray diffraction (XRD) was also conducted on the solid samples by a Bruker D2 PHASER XE-T (Bruker, Karlsruhe Germany). To study the surface functional groups, Fourier transform infrared spectra (FT-IR) was performed on the solid samples by using a Digilab FT-IR Excalibur series FTS 3000MX (Varian, Palo Alto, CA, USA) using the KBr pellet method. The X-ray photoelectron spectroscopy (XPS) was provided by an ESCALAB 250 (Thermo Electron, Waltham, MA, USA). Elemental compositions (C, H, O, N, S) of the solid samples were measured by a Vario Macro EL Analyzer (Elementar Analysensysteme GmbH, Langenselbold, Germany).

3. RESULTS AND DISCUSSION

3.1 Thermal behavior under different oxygen concentrations

As shown in Figure 2, three apparent thermal stages could be observed for the prepared samples under the four different oxygen concentrations by using thermogravimetric (TG) and differentiated thermogravimetric (DTG) analyses. The sharp mass loss at 21% O_2 around 380 to 400 °C indicated the onset of combustion, an ignition temperature (IT) for the materials could be defined in this way. For a fixed material, its IT moved to a lower temperature with the increase of oxygen concentration. The IT at the oxygen concentration of 5%, 10%, and 21% was determined to be about 375 °C, 373 °C, and 370 °C, respectively. Before the onset of ignition, a significant thermal conversion of the material occurred between 250 and 370 °C.
Here the weight loss under oxygen-free (in argon) atmosphere was significantly higher than that under any of the oxygenic conditions. This weight loss peak appeared to move towards lower temperatures with the increase of oxygen concentration, i.e., the so-called negative temperature coefficient (NTC) regime appeared to operate (25).

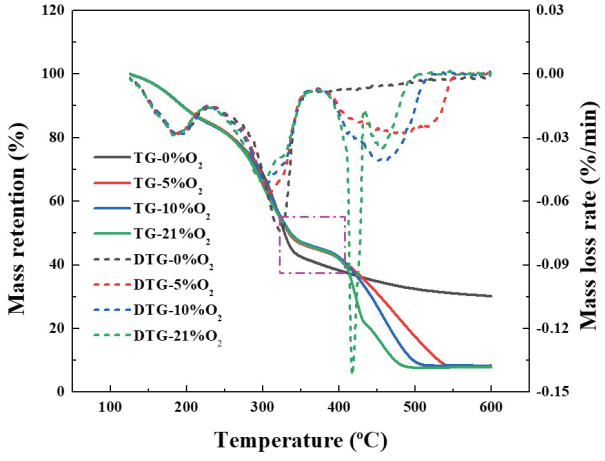


Figure 2. Thermal conversion and onset of ignition under different oxygen concentrations.

Comparing evolved products and their compositions has been an ongoing interest for different biomass conversion purposes, here specifically we were interested in the aerosol composition and their potential for inhalation in a system that removed the convective heat transfer and air exchange though the tobacco bed. It would be a process of continuous heat supply with gradually decreasing oxygen concentration. Here we adjusted the oxygen concentration flowing through the tobacco bed to further explore the effect of oxygen concentration on the auto-ignition temperature and the distribution of pyrolysis products.

The study shown in Figure 2 was designed to assess the temperature ranges where ignition could be started during thermal conversion of the material under different static oxygen concentrations. One most likely indication of sustained ignition would be substantial formation of oxides of the constituent elements, such as the oxides of carbon (CO, CO_2) and/or nitrogen (NO, NO_2). For this reason, TG-MS was subsequently performed on the sample and the results are plotted in Figure 3. It can be seen that under argon or 10% O_2 atmosphere, the CO_2 yield increased with the increase of temperature (Figure 3a). At about 200 °C, the CO_2 yield under 10% O_2 atmosphere gradually departed from the argon atmosphere and increased dramatically. At about and above 325 °C, the increase of CO_2 yield in argon atmosphere tended to stabilize. However, the CO_2 yield in 10% O_2 atmosphere exhibited a rapid surge at about 370 °C, indicating the occurrence of combustion, which was consistent with the igniting temperature of the material as tested by the DTG (Figure 2). The yield of CO under both argon and 10% O_2 atmospheres increased linearly with temperature (Figure 3b). From room temperature to 400 °C, the CO yield of 10% O_2 concentration atmosphere was always lower than that of argon atmosphere, indicating the oxidation of raw reconstituted tobacco to produce CO_2 in the presence of 10% O_2 condition. In addition, the yield of H_2O under 10% O_2 atmosphere was higher than under argon atmosphere (Figure 3c) and showed a wider temperature range of H_2O increase. Interestingly the ignition was accompanied by the second peak of H_2O production at about 370 °C in 10% O_2 atmosphere.

3.2 The composition of condensable aerosol

Permanent gas production (such as CO and CO_2) could be used to indicate and control the degree of thermal conversion and prevention of ignition, in addition the formation of condensed-phase aerosol has also been significantly affected by the oxygenation. Figure 4 shows the results of the condensed-phase substances captured by Cambridge filter pads and cold traps; they are represented by 28 volatile and semi-volatile compounds and their changes with oxygen concentrations. The captured volatile and semi-volatile organic components in Figure 4a exhibited linear or exponential growth trends with the increase of oxygen concentrations (0 to 21%), of which acrylonitrile, quinoline and isoprene showed a linear increase. The low-temperature oxidation reactions with lignocellulose biomass were usually initiated by the abstraction of an H-atom from the alkane (RH) moieties by oxygen molecules to yield alkyl (•R) and hydroperoxy (•OOH) radicals. For example, at temperatures around 327 °C, alkyl radicals are thought to react rapidly with oxygen molecules to yield peroxyalkyl radicals (ROO•), and concurrent reactions to hydroperoxide formation could lead to products such as alkenes, aldehydes, and ketones (25). This could be the reason behind the linear increase of acrylonitrile, quinoline and isoprene with oxygen concentrations. Benzene and toluene showed an exponential increase with the oxygen concentration, especially at 21% O_2 with the onset of ignition conditions. Further oxidation reactivities of benzene and toluene were thought to be extremely low at the temperature of 347 °C ~ 527 °C, due to the lack of easy isomerization of the peroxy radicals from benzene or resonance-stabilized benzylic radical for toluene (26, 27). The main reaction products were phenol and benzoic acid (from benzaldehyde), respectively. Because of the low reaction activity of benzene and toluene, the productions of phenol and benzoic acid were not sufficient to consume benzene and toluene, therefore an exponential increase with the oxygen concentrations for them were observed.

Compounds such as furans (3-furan methanol, 2(5*H*)-furanone), alcohol (propylene glycol), and ketone (1-hydroxy-2-butanone, 2,3-butanedione, cyclopentanone) made up a significant portion of condensed-phase aerosol. They also showed an increasing tendency with O_2 concentrations in Figure 4b, especially from 0% to10%.

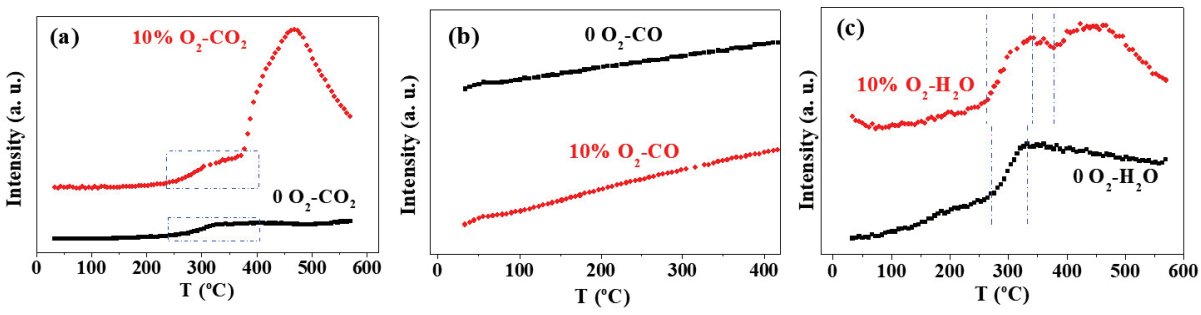


Figure 3. Thermal generation of CO, CO_2, and H_2O of the material under 0 or 10% oxygen.

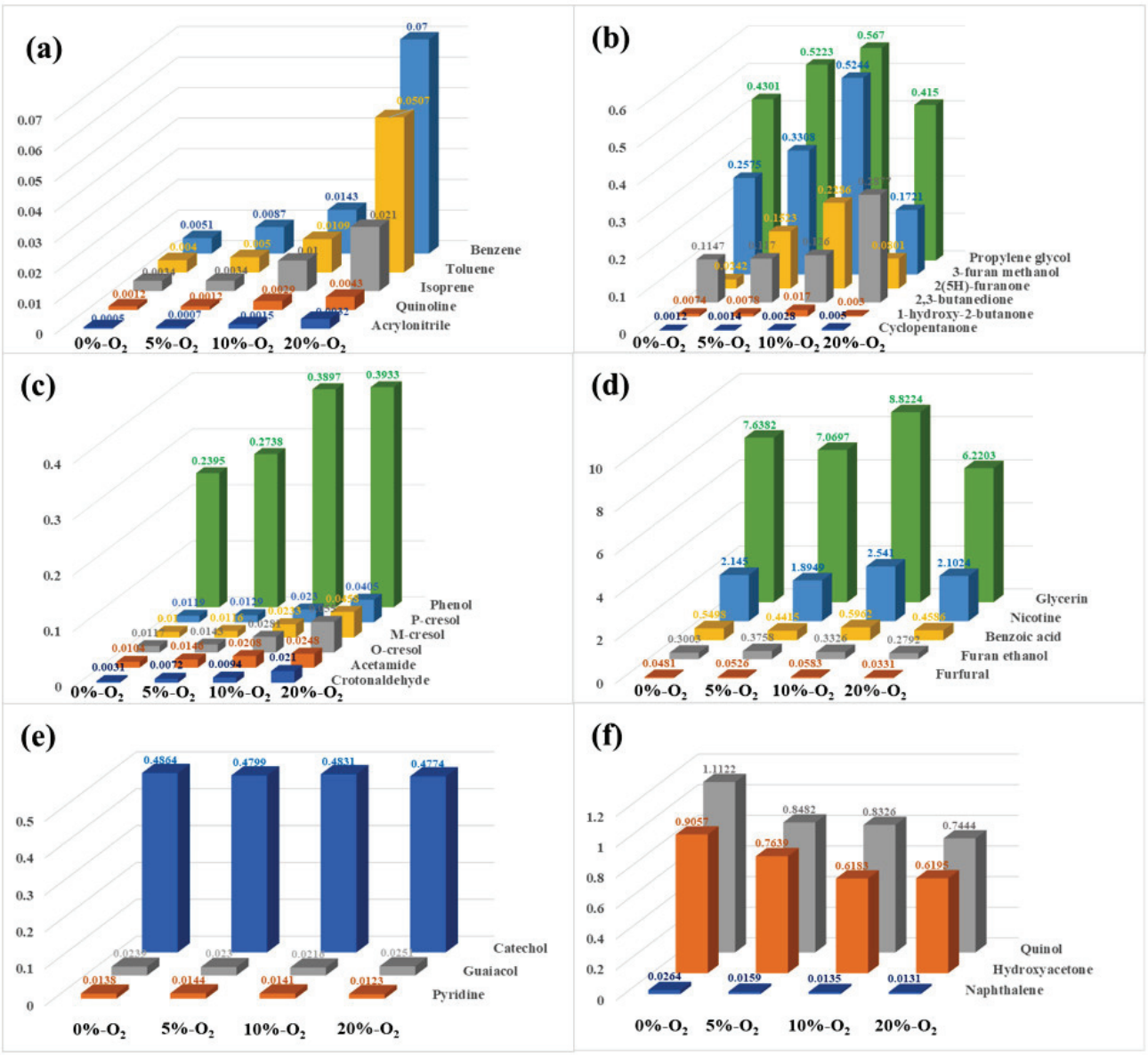


Figure 4. Pyrolysis aerosol components of samples under different oxygen concentration.

The decreasing yields of propylene glycol, 3-furan methanol, and 2(5*H*)-furanone at 21% O_2 may be the result of enhanced oxidation reaction, converting primary condensed-phase substances to secondary volatile release (28).

As shown in Figure 4c, *o*-cresol, *m*-cresol, *p*-cresol and phenol all showed an almost linear increase with increasing oxygen concentrations, illustrating that oxygen is a free radical enhancer promoting the production of this class of compounds. Within 5% – 21% O_2, the order of the linear slope was *o*-cresol > *m*-cresol > *p*-cresol. This seems to agree with the oxidization of alkylbenzenes on the benzene ring (29). Phenol increased significantly in the range of 0 – 10% oxygen concentration but not further, which might have something to do with its relative resistance the oxidation (30). Crotonaldehyde and acetamide also increased approximately linearly with the oxygen concentration.

In Figure 4d, furfural showed an initial increase followed by a decrease, exhibiting the largest yield under 10% O_2 concentration. In the literature, oxygen was shown to promote the conversion of furfural to furan under a concentration of 21%, which may explain the decrease of furfural yield (28). The remaining components in Figure 4d did not exhibit systematic changes with oxygen concentrations. The volatilization of glycerin and nicotine was known to be a thermal distillation and would not be affected by the oxygen concentrations. However, their releases may have been affected by the presence of moisture or other volatile organic components, hence they displayed a fluctuating trend with the oxygen concentrations. The fate of benzoic acid was less clear as the GC-MS method was not adequately sensitive to detect it. Catechol, guaiacol, and pyridine in Figure 4e were not oxidized or thermally destroyed within this temperature range. Naphthalene decreased with the increasing oxygen concentration (Figure 4f); it seemed oxidative decomposition of naphthalene was present but not sufficient to eliminate it. Hydroxyacetone also decreased with the increase of oxygen concentration. Reduction of hydroxyacetone in hinoki cypress sawdust and rice straw

were reported (31, 32), which was attributed to the instability of hydroxyacetone by polymerization in an oxygenated environment. The yield of quinol with the presence of oxygen was lower than under argon atmosphere and it gradually decreased with the oxygen concentration. This may have resulted from the oxygenolysis of quinol and its enhanced reaction trend with oxygen concentration (33).
In summary, some condensed-phase aerosol compounds were produced in larger quantities under the argon condition than under the oxygen condition. However, more than half of the 28 compounds showed higher yields under the oxygen atmosphere than in argon. Several volatile and semi-volatile components, phenols, aldehydes increased linearly with oxygen concentrations, even exponentially increased for benzene and toluene.

3.3 Residual solid phase products

3.3.1 Crystal structures

X-ray diffraction was used to investigate the crystal structure, crystallite size and residual strain information of materials. X-ray diffraction also allows identification and quantification of unknown phases in a mixture (34–36). X-ray diffraction (XRD) patterns in Figure 5 showed that the "γ peak" of the starting material at 15 – 22 °C disappeared gradually during the thermolysis, possibly caused by the decomposition of cellulose aliphatic hydrocarbon structure (37). Because the "γ peak" was the peak under the γ band and was caused by non-graphitic organic components (saturated structures such as aliphatic side chains). A KCl peak appeared for S-0-O and S-5-O, peaks of KCl, $CaCO_3$, $CaCl_2$ and MgO (38) appeared for S-10-O and S-21-O, and the intensity of these peaks increased with the oxygen concentrations, indicating increased oxidation of alkali metals and alkaline earth metal elements.

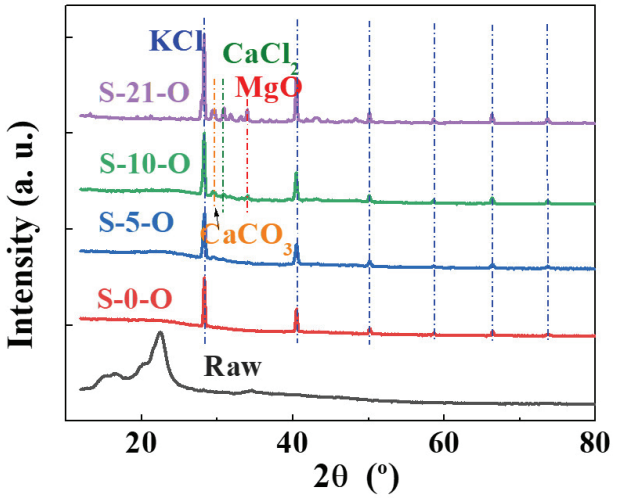


Figure 5. X-ray diffraction patterns of solid-phase products of biomass under different oxygen concentrations.

3.3.2 Elemental compositions

Elemental analysis results of S-0-O, S-5-O and S-10-O in Table 1 showed higher C, N, and S contents after thermal conversion. S-5-O exhibited more C content but less O and H contents than S-0-O, demonstrating that the oxidation reactions under 5% O_2 mainly produced H_2O or aliphatic hydrocarbon-related products. When the oxygen concentration increased to 10%, C was consumed to yield CO_2, so S-10-O showed less C and O contents than S-5-O. S-21-O possessed a low C content, consistent with the occurrence of burning under 370 °C in 21% O_2. N content increased first and then decreased with the oxygen concentrations, and S-5-O showed the highest N content, which illustrated that nitrogen-containing solid-phase products were preferentially generated under oxygen concentration of 5% and their oxidative decomposition would occur under more than 5% O_2. It could be seen from Table 1 that the sum of the percentages of these organic elements was not 100%, and the rest elements might constitute the inorganic substances that were confirmed by the X-ray diffraction results. And the sum of the percentages of organic elements in the solid-phase products gradually decreased with the increase of the oxygen concentration, indicating that the corresponding inorganic substances in the solid phase products gradually became prominent, which was consistent with the X-ray diffraction signal of the inorganic substances that gradually increased with the oxygen concentration in 3.3.1.

Table 1. Elemental analysis on solid residuals under different oxygen concentrations.

Samples	C (%)	O (%)	H (%)	N (%)	S (%)
Starting biomass	41.86	45.23	6.71	1.07	0.07
S-0-O	63.02	17.44	4.19	1.90	0.20
S-5-O	66.57	13.79	3.83	2.09	0.34
S-10-O	63.19	13.34	3.28	1.84	0.35
S-21-O	32.47	18.36	1.59	0.94	1.01

3.3.3 Surface morphology

Scanning electron microscopic pictures of the starting material and its solid phase residuals under different oxygen concentrations are shown in Figure 6. Strips of cellulosic fibers were typical of this type of engineered biomass materials, and this was the most prominent feature of all the samples. The fiber surface of the starting material was smooth (Figure 6a). With progressively higher oxygenated thermolysis, the fiber surface became rough and deposited with small particles, which indicates the beginning of structural decomposition of hemicellulose and cellulose. The degree of structural fragmentation increased with the oxygen concentrations. The large amounts of particles in S-21-O could be seen as a result of onset of ignition of the material.

3.3.4 Surface chemical composition

X-ray photoelectron spectroscopy (XPS) has proved to be one of the most powerful tools in detecting the surface structure of carbonaceous materials. Another important feature of XPS spectroscopy is the unchanged sensitivity of oxygen regardless of its chemical structures/functionality.

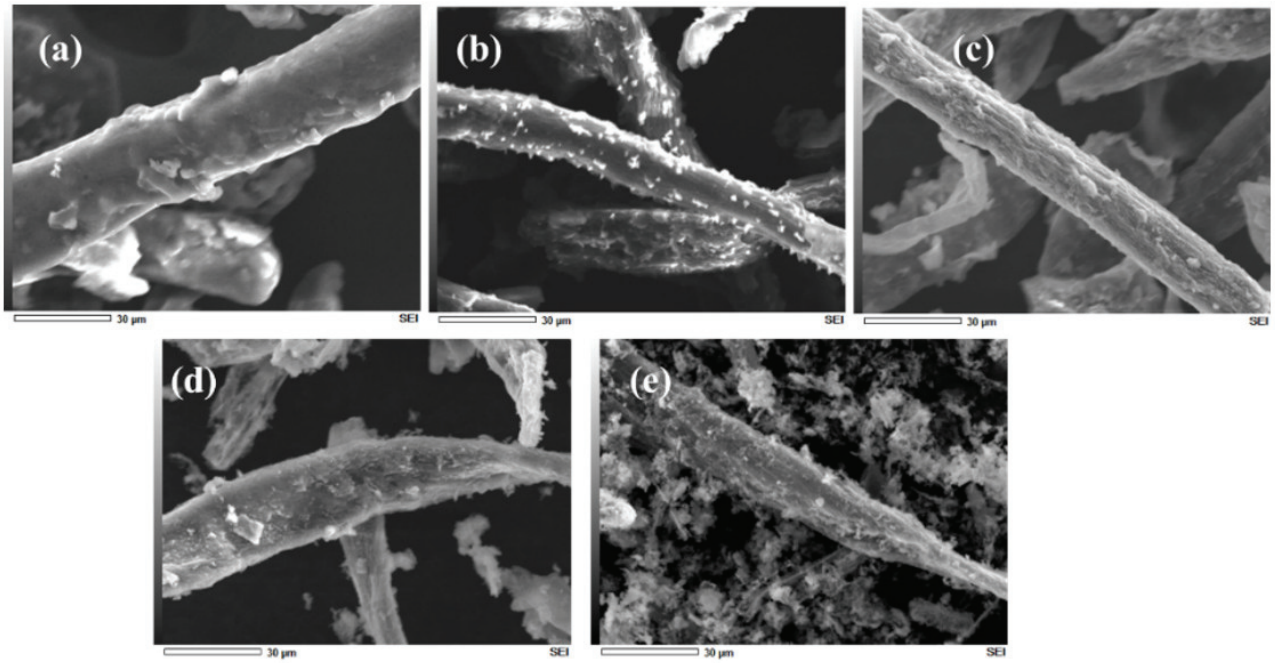


Figure 6. Morphology of the starting material and post thermal treatments (rulers were 30 µm).
(a) starting material; (b) S-0-O; (c) S-5-O; (d) S-10-O; (e) S-21-O;

This greatly facilitates the relative quantification of various classes of O-containing structures simply based on the measured peak areas. Therefore, analysis of C 1s and valence band spectra could be directed to monitor the structural evolution of the carbons in terms of extension of sp2 *vs* sp3 conjugation, carbon vacancies and oxidized carbon. Analysis of the O 1s spectra, on the other hand, provided a tool to characterize the nature of oxygen bonding on carbon and to determine the relative abundance of carbon-oxygen species (39–41). X-ray photoelectron spectroscopy results of the starting material in Figure 7a showed three main types of carbon configurations at 284.8, 286.0, and 287.3 eV; they were ascribed to C-H/C-C, C-O/C-O-C and O-C-O/C=O, respectively, deduced from hemicellulose and cellulose components. S-0-O showed the same three types of carbon configurations with the starting material (Figure 7b), but showed less C-H/C-C, C-O/C-O-C (Table 2) due to the dehydroxylation and decarboxylation of hemicellulose and cellulose. The C-H/C-C became less and less with increase of oxygen concentration from S-5-O to S-10-O to S-21-O (Figures 7 (c, d, e) and Table 2). In addition to C-H/C-C, C-O/C-O-C, O-C-O/C=O, S-5-O, S-10-O and S-21-O also formed a little -O-C=O, resulting from the oxidation of C-H/C-C. Maybe the oxidation reaction under the different oxygen concentrations promoted the oxidation reaction of C-H/C-C to form -O-C=O and afterwards H_2O and CO_2 and suppressed the thermal decomposition reaction at the same time (42).
From X-ray photoelectron spectroscopy O 1s of the starting material in Figure 8(a), the large peak at 532.2 eV was ascribed to C-OH/C-O-C and the other one at 531.0 eV was ascribed to C=O (43), and the aera of C-OH/C-O-C decreased drastically when being heated at 370 °C under argon atmosphere by dehydroxylation (Figure 8(b) and Table 3).

Table 2. The relative percentage of surface carbon-containing functional groups by X-ray photoelectron spectroscopy.

Samples	Content of functional groups (%)			
	C-H/C-C	C-O/C-O-C	O-C-O/C=O	-O-C=O
Starting material	75.47	17.78	6.76	–
S-0-O	87.79	7.59	4.62	–
S-5-O	80.84	5.75	9.58	3.82
S-10-O	78.56	9.04	9.03	3.37
S-21-O	74.88	9.96	8.67	6.49

The result was consistent with the above H and O element analysis results of S-0-O and the starting material. Just like with S-0-O, the solid residual products under the oxygen atmosphere also exhibited increased C=O and decreased C-OH/C-O-C when compared with the starting material (Figures 8 (c, d, e)). Moreover, the oxygen-containing groups (e.g., C-OH/C-O-C and C=O) also increased with the oxygen concentration for S-5-O to S-10-O to S-21-O. Therefore, the oxidation of the biomass resulted in oxygen loading on the solid surface and suppressed thermal decomposition.

3.3.5 FT-IR analysis

As shown in Figure 9, -OH and C-H (bands at 3400 – 3200 cm^{-1} and 2900 – 2800 cm^{-1}) of the starting material almost disappeared when being heated at the different oxygen concentrations, indicating the dehydroxylation and decomposition of hemicellulose and cellulose. With increase of the oxygen concentrations, the C=C at 1600 cm^{-1} also became weaker from S-0-O to S-21-O. On the other hand, the -COO (1650 – 1505 cm^{-1}) and C-O-C

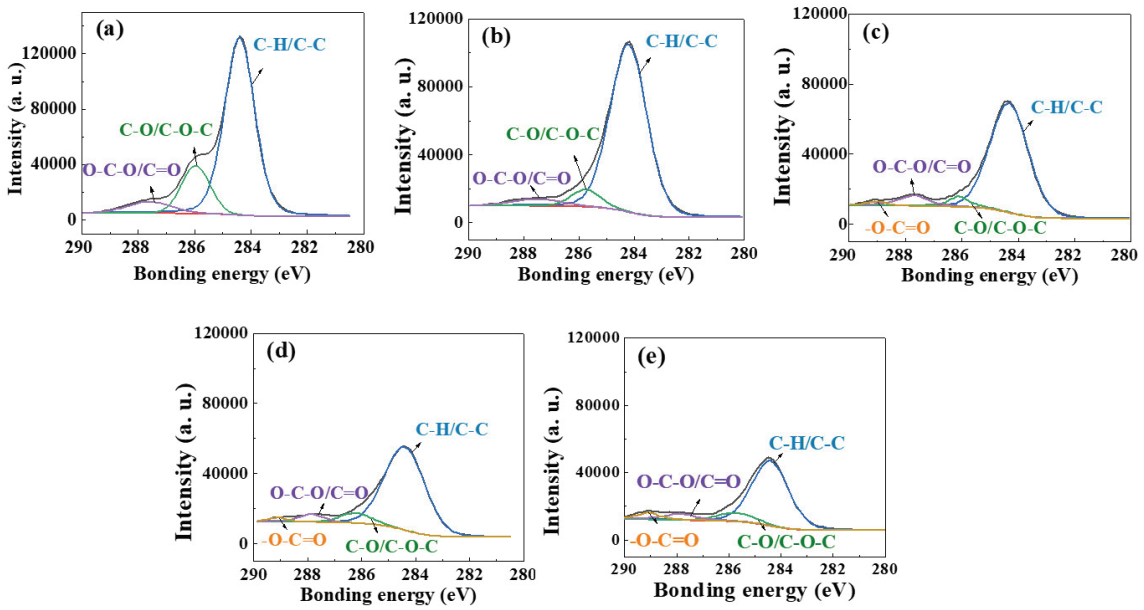


Figure 7. High-resolution X-ray photoelectron spectrum of C 1s peak.
(a) Starting material; (b) S-0-O; (c) S-5-O; (d) S-10-O; (e) S-21-O;

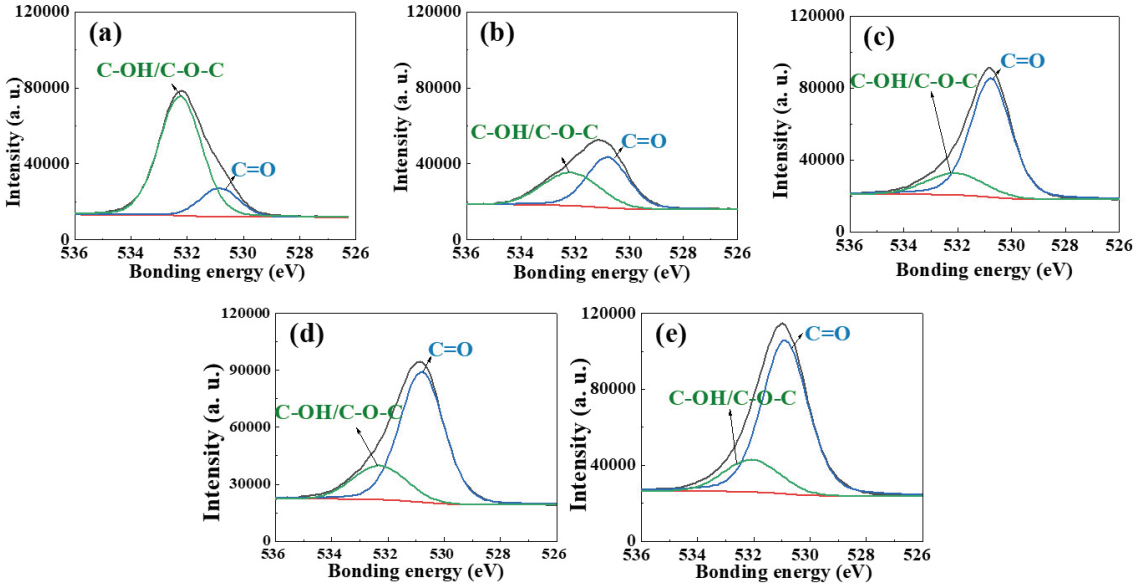


Figure 8. High-resolution X-ray photoelectron spectrum of O 1s peak.
(a) Starting material; (b) S-0-O; (c) S-5-O; (d) S-10-O; (e) S-21-O;

Table 3. The relative percentage of surface oxygen-containing functional groups by X-ray photoelectron spectroscopy.

Samples	Content of the functional groups (%)	
	C=O	C-O-C/C-OH
Raw reconstituted tobacco	17.58	82.42
S-0-O	69.08	30.92
S-5-O	73.43	26.57
S-10-O	72.46	27.54
S-21-O	81.37	18.63

(900 – 700 cm^{-1}) increased gradually with the rising oxygen concentration. In addition, the variation of C-O-C could possibly be explained by consecutive reaction pathways, a decomposition followed by an oxygenation synthesis.

4. CONCLUSIONS

A systematic investigation of oxygenated thermal conversion on an engineered biomass material was conducted, including gaseous and volatile products, condensed-phase aerosol products and solid residuals. Attention was paid to

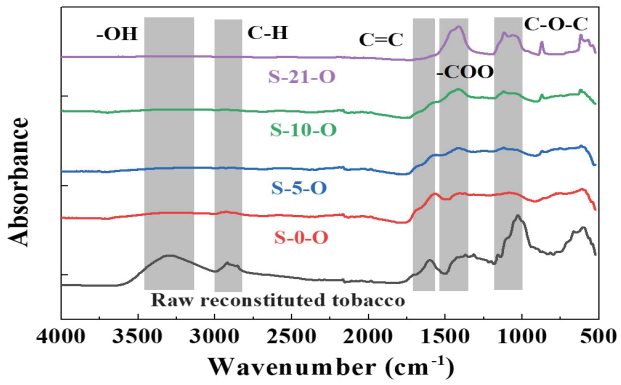


Figure 9. FT-IR spectra of solid residuals under different oxygen concentrations.

four different oxygen concentrations (0, 5%, 10% and 21%) at a temperature below 370 °C to avoid ignition of the starting material. The ignition temperature of the material decreased with the oxygen concentration and the NTC was observed under the different oxygen atmospheres at the temperature range. More CO_2 and less CO yielded for oxygenic atmosphere than inert atmosphere, and more aerosols were produced under the inert atmosphere than under oxygenated conditions. Lower oxygen concentrations were beneficial to the yields of condensable aerosol components. Some compounds (e.g., phenols, aldehydes) showed better yields under the oxygen atmosphere, supported by gas-phase oxidative formation. In addition, higher oxygen concentrations also resulted in larger bulk and surface oxygen contents for the solid residual. The contents of inorganic compounds also exhibited an increase with oxygen concentrations. This study provided basic and useful information to the design of suitable thermal biomass conversion, aimed at producing controlled condensable aerosol phase products.

ABBREVIATIONS

Abbreviation	Corresponding full wording or explanatory wording
NSC	a label of our novel-designed airflow pathway of heated tobacco products (18)
NTC	negative temperature coefficient
TG	thermogravimetric
DTG	derivative thermogravimetric
GC-MS	gas chromatography-mass spectrometry
SEM	scanning electron microscope
XRD	X-ray diffraction
FT-IR	Fourier transform infrared spectra
XPS	X-ray photoelectron spectroscopy
IT	ignition temperature
TG-MS	thermogravimetric analyser with a mass spectrometer

REFERENCES

1. Baker, R.R.: Smoke Generation Inside a Burning Cigarette: Modifying Combustion to Develop Cigarettes That may be Less Hazardous to Health; Prog. Energy Combust. Sci. 32 (2006) 373–385. DOI: 10.1016/j.pecs.2006.01.001
2. Health Canada: Tobacco Reporting Regulations; SOR/2000-273, Schedule 2 (2000). Available at: https://laws-lois.justice.gc.ca/eng/regulations/SOR-2000-273/index.html (accessed October 2022)
3. World Health Organization (WHO): The Scientific Basis of Tobacco Product Regulation: Report of the WHO Study Group (TobReg); Technical Report Series 951, WHO, Geneva, Switzerland, 2008.
4. U.S. Food and Drug Administration (FDA): Harmful and Potentially Harmful Constituents in Tobacco Products and Tobacco Smoke; Established List; Federal Register Food and Drug Administration 77 (2012) p. 20034.
5. Torikai, K., S. Yoshida, and H. Takahashi: Effects of Temperature, Atmosphere and pH on the Generation of Smoke Compounds During Tobacco Pyrolysis; Food Chem. Toxicol. 42 (2004) 1409–1417. DOI: 10.1016/j.fct.2004.04.002
6. R.J. Reynolds Tobacco Company: Chemical and Biological Studies on New Cigarette Prototypes That Heat Instead of Burn Tobacco; R.J. Reynolds Tobacco Co., Winston-Salem, NC 27102, USA, 1988.
7. Stabbert, R., P. Voncken, K. Rustemeier, H.J. Haussmann, E. Roemer, H. Schaffernicht, and G. Patskan: Toxicological Evaluation of an Electrically Heated Cigarette. Part 2: Chemical Composition of Mainstream Smoke; J. Appl. Toxicol. 23 (2003) 329–339. DOI: 10.1002/jat.924
8. Tewes, F.J., T.J. Meisgen, D.J. Veltel, E. Roemer, and G. Patskan: Toxicological Evaluation of an Electrically Heated Cigarette. Part 3: Genotoxicity and Cytotoxicity of Mainstream Smoke; J. Appl. Toxicol. 23 (2003) 341–348. DOI: 10.1002/jat.925
9. Patskan, G. and W. Reininghaus: Toxicological Evaluation of an Electrically Heated Cigarette. Part 1: Overview of Technical Concepts and Summary of Findings; J. Appl. Toxicol. 23 (2003) 323–328. DOI: 10.1002/jat.923
10. Schorp, M.K., A.R. Tricker, and R. Dempsey: Reduced Exposure Evaluation of an Electrically Heated Cigarette Smoking System. Part 1: Non-Clinical and Clinical Insights; Regul. Toxicol. Pharmacol. 64 (2012) S1–S10. DOI: 10.1016/j.yrtph.2012.08.008
11. Wynder E.L., G. Wright, and J. Lam: A Study of Tobacco Carcinogenesis. V. The Role of Pyrolysis; Cancer 11 (1958) 1140–1148. DOI: 10.1002/1097-0142(195811/12)11:6<1140::AID-CNCR2820110609>3.0.CO;2-Z
12. White, J.L., B.T Connor, T.A. Perfetti, B.R. Bombick, J.T. Avalos, K.T. Fowler, C.J. Smith, and D.J. Doolittle: The Effect of Pyrolysis Temperature on Mutagenicity of Tobacco Smoke Condensate; Food Chem. Toxicol. 39 (2001) 499–505. DOI: 10.1016/S0278-6915(00)00155-1
13. Cozzani, V., T. Mc Grath, M. Smith, J.-P. Schaller, and

G. Zuber: Absence of Combustion in an Electrically Heated Tobacco System - An Experimental Investigation; presented at the 21st International Symposium on Analytical and Applied Pyrolysis, Nancy, France. 9th–12th May 2016. Available at: https://www.pmiscience.com/content/dam/pmiscience/en/publications/presentations-and-posters/pdf/absence-of-combustion-in-an-electrically-heated-tobacco-system-an-experimental-investigation-(1).pdf
14. Bentley, M.: What do we Know About the Chemistry of IQOS Aerosol?; Philip Morris International, PMI Science, 2020. Available at: https://www.pmiscience.com/Open-Science/september-open-science-presentations/bentley-chemistry-iqos- aerosol (accessed October 2022)
15. Horinouchi, T. and S. Miwa: Comparison of Cytotoxicity of Cigarette Smoke Extract Derived from Heat-Not-Burn and Combustion Cigarettes in Human Vascular Endothelial Cells; J. Pharmacol. Sci. 147 (2021) 223–233. DOI: 10.1016/j.jphs.2021.07.005.
16. Eaton, D., B. Jakaj, M. Forster, J. Nicol, E. Mavropoulou, K. Scott, C. Liu, K. McAdam, J. Murphy, and C.J. Proctor: Assessment of Tobacco Heating Product THP1.0. Part 2: Product Design, Operation and Thermophysical Characterisation; Regul. Toxicol. Pharmacol. 93 (2018) 4–13. DOI: 10.1016/j.yrtph.2017.09.009
17. Lee, J. and S. Lee: Korean-Made Heated Tobacco Product, 'Lil'; Tob. Control 0 (2018) 1–2. DOI: 10.1136/tobaccocontrol-2018-054430
18. Li, B., Y. Sun, L. Fu, L. Feng, P. Lei, C. Liu, J. Han, S. Shang, S. Wang, L. Wang, Y. Pan, Q. Zhang, Z. Guo, F. Huang, M. Zhang, J. Tang, B. Wang, and K. Zhang: Aerosol Formation and Transfer in Open- and not Open-Ended Heated Tobacco Products; Contrib. Tob. Nicotine Res. 31 (2022) 162–174. DOI: 10.2478/cttr-2022-0017
19. Sun, T., C. Sun, Q. Song, Y. Li, X. Wang, and X. Shu: Strengthening the Results of Destroying the Caking Property of CBC in Weak Oxygen and Upgrading Pyrolysis Products; Fuel 205 (2017) 90–99. DOI: 10.1016/j.fuel.2017.05.040
20. Rashid Khan, M., R. Usmen, E. Newton, S. Beer, and W. Chisholm: E.S.R. Spectroscopic Study on the Chemistry of Coal Oxidation; Fuel 67 (1988) 1668–1673. DOI: 10.1016/0016-2361(88)90213-X
21. Busch, C., T. Streibel, C. Liu, K.G. McAdam, and R. Zimmermann: Pyrolysis and Combustion of Tobacco in a Cigarette Smoking Simulator Under Air and Nitrogen Atmosphere; Anal. Bioanal. Chem 403 (2012) 419–430. DOI: 10.1007/s00216-012-5879-9
22. Senneca, O., S. Ciaravolo, and A. Nunziata: Composition of the Gaseous Products of Pyrolysis of Tobacco Under Inert and Oxidative Conditions; J. Anal. Appl. Pyrolysis 79 (2007) 234–243. DOI: 10.1016/j.jaap.2006.09.011
23. Alderman, S.L., C. Song, S.C. Moldoveanu, and S.K. Cole: Particle Size Distribution of E-Cigarette Aerosols and the Relationship to Cambridge Filter Pad Collection Efficiency; Beitr. Tabakforsch. Int. 26 (2014) 183–190. DOI: 10.1515/cttr-2015-0006
24. Hofer, I., L. Gautier, E. Cortes Sauteur, M. Dobler, A. Python, C. O'Reilly, D. Gisi, Daniel, E. Tinguely, L. Wehren, and E. García Fidalgo: A Screening Method by Gas Chromatography-Mass Spectrometry for the Quantification of 24 Aerosol Constituents From Heat-Not-Burn Tobacco Products; Beitr. Tabakforsch. Int. 28 (2019) 317–328. DOI: 10.2478/cttr-2019-0013
25. Herbinet, O. and F. Battin-Leclerc: Progress in Understanding Low-Temperature Organic Compound Oxidation Using a Jet-Stirred Reactor; Int. J. Chem. Kinet. 46 (2014) 619–639. DOI: 10.1002/kin.20871
26. Herbinet, O., B. Husson, M. Ferrari, P.A. Glaude, and F. Battin-Leclerc: Low Temperature Oxidation of Benzene and Toluene in Mixture With *n*-Decane; Proc. Combust. Inst. 34 (2013) 297–305. DOI: 10.1016/j.proci.2012.06.005
27. Bounaceur, R., I. Da Costa, R. Fournet, F. Billaud, and F. Battin-Leclerc: Experimental and Modeling Study of the Oxidation of Toluene; Int. J. Chem. Kinet. 37 (2005) 25–49. DOI: 10.1002/kin.20047
28. Zhao, S., Y. Luo, Y. Su, Y. Zhang, and Y. Long: Experimental Investigation of the Oxidative Pyrolysis Mechanism of Pinewood on a Fixed-Bed Reactor; Energy Fuels 28 (2014) 5049–5056. DOI: 10.1021/ef500612q
29. Roubaud, A., O. Lemaire, A. Minetti, and L.R. Sochet: High Pressure Auto-Ignition and Oxidation Mechanisms of *o*-Xylene, *o*-Ethyltoluene, and *n*-Butylbenzene Between 600 and 900 K; Combust. Flame 123 (2000) 561–571. DOI: 10.1016/S0010-2180(00)00174-7
30. Li, D., F. Berruti, and C. Briens: Autothermal Fast Pyrolysis of Birch Bark with Partial Oxidation in a Fluidized Bed Reactor; Fuel 121 (2014) 27–38. DOI: 10.1016/j.fuel.2013.12.042
31. Yi, S., Y. Luo, C. Yi, W. Wu, and Y. Zhang: Experimental and Numerical Investigation of Tar Destruction Under Partial Oxidation Environment; Fuel Process. Technol. 92 (2011) 1513–1524. DOI: 10.1016/j.fuproc.2011.03.013
32. Zhang, Y., S. Kajitani, M. Ashizawa, and Y. Oki: Tar Destruction and Coke Formation During Rapid Pyrolysis and Gasification of Biomass in a Drop-Tube Furnace; Fuel 89 (2010) 302–309. DOI: 10.1016/j.fuel.2009.08.045
33. Ogunlaja, A.S., M.S. Abdul-Quadir, P.E. Kleyi, E.E. Ferg, P. Watts, and Z.R. Tshentu: Towards Oxidative Denitrogenation of Fuel Oils: Vanadium Oxide-Catalysed Oxidation of Quinoline and Adsorptive Removal of Quinoline-N-oxide using 2,6-Pyridine-polybenzimidazole Nanofibers; Arab. J. Chem. 12 (2019) 198–214. DOI: 10.1016/j.arabjc.2017.05.010
34. Cetin, E., B. Moghtaderi, R. Gupta, and T.F. Wall: Influence of Pyrolysis Conditions on the Structure and Gasification Reactivity of Biomass Chars; Fuel 83 (2004) 2139–2150. DOI: 10.1016/j.fuel.2004.05.008
35. Lu, L., V. Sahajwalla, C. Kong, and D. Harris: Quantitative X-Ray Diffraction Analysis and its Application to Various Coals; Carbon 39 (2001) 1821–1833. DOI: 10.1016/S0008-6223(00)00318-3
36. Schoening, F.R.L.: X-Ray Structure of Some South African Coals Before and After Heat Treatment at 500 and 1000 °C; Fuel 62 (1983) 1315–20. DOI: 10.1016/S0016-2361(83)80016-7
37. Liu, R.: Research on Biomass Oxidative Torrefaction and Combustion Properties; PhD Thesis, Huazhong University of Science and Technology, Wuhan, China, 2014.

38. Yan, J., Z. Lei, Z. Li, Z. Wang, S. Ren, S. Kang, X. Wang, and H. Shui: Molecular Structure Characterization of Low-Medium Rank Coals via XRD, Solid State ^{13}C NMR and FTIR Spectroscopy; Fuel 268 (2020) 117038. DOI: 10.1016/j.fuel.2020.117038
39. Wang, S., L. Wu, X. Hu, L. Zhang, K.M. O'Donnell, C.E. Buckley, and C. Li: An X-Ray Photoelectron Spectroscopic Perspective for the Evolution of O-Containing Structures in Char During Gasification; Fuel Process. Technol. 172 (2018) 209–215. DOI: 10.1016/j.fuproc.2017.12.019.
40. Perry, D.L. and A. Grint: Application of XPS to Coal Characterization, Fuel 62 (1983) 1024–1033. DOI: 10.1016/0016-2361(83)90135-7
41. Gardner, S.D., C.S.K. Singamsetty, G.L. Booth, G.-R. He, and C.U. Pittman: Surface Characterization of Carbon Fibers Using Angle-Resolved XPS and ISS; Carbon 33 (1995) 587–595. DOI: 10.1016/0008-6223(94)00144-O
42. Cerciello, F., O. Senneca, A. Coppola, A. Forgione, P. Lacovig, and P. Salatino: The Influence of Temperature on the Nature and Stability of Surface-Oxides Formed by Oxidation of Char; Renew. Sustain. Energy Rev. 137 (2021) 110595. DOI: 10.1016/j.rser.2020.110595
43. Liang, J.Y., T.T. Qu, K. Xiang, Y. Zhang, S.Y. Chen, Y.C. Cao, M.J. Xie, and X.F. Guo: Microwave Assisted Synthesis of Camellia Oleifera Shell-Derived Porous Carbon with Rich Oxygen Functionalities and Superior Supercapacitor Performance; Appl. Surf. Sci. 436 (2018) 934–940. DOI: 10.1016/j.apsusc.2017.12.142

Corresponding author:

Bin Li, Ph.D.
Zhengzhou Tobacco Research Institute of CNTC
Zhengzhou 450001
Henan, China
E-mail: ztrilibin@163.com